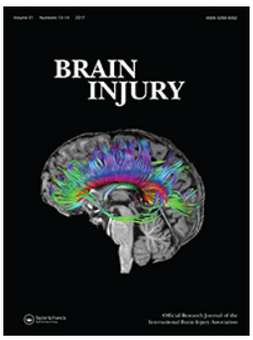

Brain Injury

ISSN: 0269-9052 (Print) 1362-301X (Online) Journal homepage: http://www.tandfonline.com/loi/ibij20

A pilot treatment study for mild traumatic brain injury: Neuroimaging changes detected by MEG after low-intensity pulse-based transcranial electrical stimulation

Ming-Xiong Huang, Ashley Robb Swan, Annemarie Angeles Quinto, Scott Matthews, Deborah L. Harrington, Sharon Nichols, Barry J. Bruder, Corey C. Snook, Charles W. Huang, Dewleen G. Baker & Roland R. Lee

To cite this article: Ming-Xiong Huang, Ashley Robb Swan, Annemarie Angeles Quinto, Scott Matthews, Deborah L. Harrington, Sharon Nichols, Barry J. Bruder, Corey C. Snook, Charles W. Huang, Dewleen G. Baker & Roland R. Lee (2017) A pilot treatment study for mild traumatic brain injury: Neuroimaging changes detected by MEG after low-intensity pulse-based transcranial electrical stimulation, Brain Injury, 31:13-14, 1951-1963, DOI: 10.1080/02699052.2017.1363409

To link to this article: https://doi.org/10.1080/02699052.2017.1363409

BRAIN INJURY
2017, VOL. 31, NOS. 13–14, 1951–1963
https://doi.org/10.1080/02699052.2017.1363409

Taylor & Francis
Taylor & Francis Group

A pilot treatment study for mild traumatic brain injury: Neuroimaging changes detected by MEG after low-intensity pulse-based transcranial electrical stimulation

Ming-Xiong Huang[a,b]*, Ashley Robb Swan[a,b], Annemarie Angeles Quinto[a,b], Scott Matthews[c,d], Deborah L. Harrington[a,b], Sharon Nichols[e], Barry J. Bruder[f], Corey C. Snook[g], Charles W. Huang[h], Dewleen G. Baker[a,i,j], and Roland R. Lee[a,b]

[a]Radiology, Research, and Psychiatry Services, VA San Diego Healthcare System, San Diego, CA, USA; [b]Department of Radiology, University of California San Diego, La Jolla, CA, USA; [c]Department of Psychiatry, University of California San Diego, La Jolla, CA, USA; [d]ASPIRE Center, VASDHS Residential Rehabilitation Treatment Program, San Diego, CA, USA; [e]Department of Neurosciences, University of California San Diego, La Jolla, CA, USA; [f]IASIS Technologies, Inc. Los Angeles, CA, USA; [g]Mind-Brain Training Institute, Mount Dora, FL, USA; [h]Department of Bioengineering, University of California San Diego, La Jolla, CA, USA; [i]Department of Psychiatry, University of California San Diego, La Jolla, CA, USA; [j]VA Center of Excellence for Stress and Mental Health, San Diego, CA, USA

ABSTRACT

Background: Mild traumatic brain injury (mTBI) is a leading cause of sustained impairments in military service members, Veterans, and civilians. However, few treatments are available for mTBI, partially because the mechanism of persistent mTBI deficits is not fully understood.

Methods: We used magnetoencephalography (MEG) to investigate neuronal changes in individuals with mTBI following a passive neurofeedback-based treatment programme called IASIS. This programme involved applying low-intensity pulses using transcranial electrical stimulation (LIP-tES) with electroencephalography monitoring. Study participants included six individuals with mTBI and persistent post-concussive symptoms (PCS). MEG exams were performed at baseline and follow-up to evaluate the effect of IASIS on brain functioning.

Results: At the baseline MEG exam, all participants had abnormal slow-waves. In the follow-up MEG exam, the participants showed significantly reduced abnormal slow-waves with an average reduction of 53.6 ± 24.6% in slow-wave total score. The participants also showed significant reduction of PCS scores after IASIS treatment, with an average reduction of 52.76 ± 26.4% in PCS total score.

Conclusions: The present study demonstrates, for the first time, the neuroimaging-based documentation of the effect of LIP-tES treatment on brain functioning in mTBI. The mechanisms of LIP-tES treatment are discussed, with an emphasis on LIP-tES's potentiation of the mTBI healing process.

KEYWORDS

Flexyx neurotherapy system; low energy neurofeedback system; magnetoencephalography; slow-wave

Introduction

Background

Traumatic brain injury (TBI) is a leading cause of sustained physical, cognitive, emotional, and behavioural deficits in the civilian population and military personnel. The majority of TBIs are in the 'mild' range of severity. Mild TBI (mTBI) accounts for 75% of civilian TBIs from motor vehicle accidents, sports, falls, and assaults (1). In active-duty military personnel and combat Veterans, the majority (89%) of TBIs from blast injuries are also mild (2). However, the pathophysiology of mTBI is not completely understood and the long-term effects of mTBI are controversial. In the majority of individuals with mTBI, symptoms resolve within days post injury (3). Yet, post-concussive symptoms (PCS) can persist for 3 months post injury or longer, indicating chronic sequelae. Estimates of the prevalence of persistent PCS vary widely. In a general civilian population, between 8% and 33% patients with mTBI show persistent long-term cognitive and/or behavioural impairments (4–10). In Veterans with combat-related mTBI, at least three enduring PCS were reported in 7.5–40% of patients (11–14). It is unknown why similar acute mTBI events can lead to dramatic neurobehavioural decompensation with persistent PCS in some individuals, but not in others (15). Optimal rehabilitation treatments for chronic PCS in mTBIs are also not understood, owing to insufficient information about the loci and mechanisms of injuries and the absence of neuroimaging-based assessments of treatment efficacy.

Transcranial electrical stimulation for mTBI

A promising class of treatments for mTBI is passive neurofeedback that applies low-intensity pulses using transcranial electrical stimulation (LIP-tES) with electroencephalography (EEG) monitoring. This class of EEG neurofeedback treatments use a common hardware design, but different software/protocol approaches; examples include Low Energy Neurofeedback System (LENS) (16), Flexyx Neurotherapy System (FNS) (17), and IASIS (the Greek word for healing or cure) (18). It is suggested that these treatments offset brainwave activity by applying LIP-tES using the same EEG cables

CONTACT Ming-Xiong Huang Professor mxhuang@ucsd.edu Radiology Imaging Laboratory, University of California at San Diego, 3510 Dunhill Street, San Diego, CA 92121, USA.

Color versions of one or more of the figures in the article can be found online at www.tandfonline.com/IBIJ.

and electrodes that measure the brain waves (19). LENS and FNS have been used to treat individuals with TBI, including mTBI, showing positive effects on behavioural sequelae (19–23). In addition, Larsen and colleagues reported that neurofeedback treatment significantly decreased EEG amplitude at the highest amplitude electrode site and at electrode Cz in a mixed population of individuals with TBI and other disorders (20). It was not clear exactly why LIP-tES pulses were beneficial, though it was perceived that LIP-tES can offset the brain waves from its dominant frequency, presumably in an abnormal state (16,20). However, the underlying mechanism(s) of efficacy of LIP-tES treatment in TBI are not understood, nor have they been studied in animal models. No neuroimaging studies have assessed neuronal changes in the brain after LIP-tES treatment in individuals with TBI, and their relationship to improved behavioural outcomes.

MEG as a biomarker for mTBI

In this regard, magnetoencephalography (MEG) is of keen interest because it is a non-invasive functional imaging technique that directly measures the neuronal current in grey matter (GM) with high temporal resolution (<1 ms) and good spatial localization accuracy (2–3 mm at cortical level) (24). MEG is highly sensitive to abnormal slow-wave signals in mTBI (delta-band 1–4 Hz, extending to theta-band 5–7 Hz) (25–31). Slow-waves, if present during wakefulness, are a sign of brain dysfunction (32). Neurophysiological studies in animals have established a solid connection between pathological delta-wave (1–4 Hz) generation in GM and injuries in white matter (WM). Polymorphic delta-band slow-waves produced by WM axonal lesions in cats were localized to the GM of cortex overlying the lesion (33,34). Abnormal delta-waves can also be induced by the administration of atropine in WM (35). It is known that atropine is a competitive antagonist of acetylcholine (ACh) receptors and can block and/or limit ACh. These animal experiments concluded that cortical deafferentation was a key factor in abnormal delta-wave production in GM, owing to WM lesions (i.e. axonal injury) and/or blockages/limitations in the cholinergic pathway (36). Using diffusion tensor imaging (DTI), it was found that abnormalities in underlying WM tracts in some individuals with mTBI were related to abnormal MEG slow-waves in GM (25). Sleep studies further support the relationship between delta-wave generation and cholinergic blockage/limitation. During REM sleep and awake stages, the brain rhythms are dominated by oscillations at a frequency higher than that of delta waves. However during non-REM sleep stages 3 and 4, delta-waves are the dominant brain rhythm in the brain. ACh is one of the leading neurotransmitters related to sleep. ACh neurotransmitter affects certain cholinergic neurons that are active strongly during periods of REM sleep, but much less so during non-REM sleep and therefore are called REM-ON cells (37). The marked reduction/limitation of ACh release during the non-REM sleep stages 3 and 4 is a key contributor to the pronounced generation of delta waves during those stages (32).

Evidence is mounting in support of resting-state MEG (rs-MEG) slow-wave source imaging during wakefulness as a non-invasive imaging marker for neuronal abnormalities in mTBI (25–31). Using region of interest (ROI) and voxel-wise approaches, it was demonstrated that rs-MEG slow-wave source imaging detects abnormal slow-waves (delta-band, 1–4 Hz) with ~85% sensitivity in patients with chronic or sub-acute mTBI who also had persistent PCS (26,27).

Purpose

The present study used rs-MEG to identify functional mechanisms associated with twice-weekly IASIS treatments for 6 weeks in individuals with chronic mTBI and persisting PCS. MEG source imaging changes in abnormal slow-waves were studied before and after IASIS treatments in participants with mTBI. In addition, we examined whether changes in PCS after treatments were associated with changes in abnormal MEG slow-waves. Our main hypothesis was that IASIS treatment would be associated with significant decreases in both abnormal MEG slow-waves and PCS in individuals with mTBI relative to the pre-treatment baseline. We also predicted that MEG slow-wave changes would correlate with changes in PCS.

Methods and materials

The study protocol was approved by institutional review boards of the University of California, San Diego. All participants gave written informed consent prior to study procedures. The informed consent followed the ethical guidelines of the Declarations of Helsinki (sixth revision, 2008).

Research participants

Table 1 describes demographic and clinical characteristics of the six study participants. All participants had a chronic mTBI

Table 1. Demographic and clinical characteristics of six participants with mTBI.

Information	Participant #1	Participant #2	Participant #3	Participant #4	Participant #5	Participant #6
Age	40	41	29	27	28	33
Education (yrs)	12	14	14	13	12	12
Gender	M	F	M	M	M	M
Total No. mTBI	1	3	1	1	2	More than 3
†mTBI Type	Blast	MVA	MVA	Blast	Blunt impact	Blast
†PCS Duration (months)	28	14	46	51	66	84
†LOC	>10 s	10 min	Dazed	Dazed	10 s	2–15 min
†PTA	1–24 h	1–24 h	>1 min	>1 min	1–24 h	16 min–1 h
Medications	N/A	1 SSRI	N/A	N/A	N/A	1 SSRI

†For the most recent mTBI, LOC = loss of consciousness; PCS = post-concussive symptoms; PTA = post-traumatic amnesia.

with persistent PCS for an average of 48.2 (± 25.2) months between the most recent mTBI and the baseline interview (see below). Three participants had multiple mTBIs. For the most recent incident, causes of injury included blast (n = 3), motor vehicle accident (MVA; n = 2), and blunt trauma (n = 1).

Participants were evaluated in a baseline interview to assess the nature of their injuries and persistent PCS. The diagnosis and classification of mTBI in the participants were based on standard VA and Department of Defense (DOD) diagnostic criteria (38): 1) loss of consciousness (LOC) < 30 minutes or transient confusion, disorientation, or impaired consciousness immediately after the trauma; 2) post-traumatic amnesia (PTA) < 24 hours; and 3) initial Glasgow Coma Scale (GCS) (39) between 13–15 (if available). Since the GCS assessment was often not available, individuals with missing GCS, but who met other inclusion criteria, were also enrolled. Table 1 lists the LOC and PTA information for the most recent mTBI, and the total number of TBIs for each participant.

In addition, these participants did not meet the typical exclusion criteria used in MEG studies for mTBI (26,27,31): 1) history of other neurological, developmental, or psychiatric disorders (e.g. brain tumour, stroke, epilepsy, Alzheimer disease, or schizophrenia, bipolar disorder, attention deficit hyperactivity disorder, or diagnosis of learning disability); 2) diagnosis of major depressive disorder (MDD) prior to the mTBI; 3) substance or alcohol use disorder according to DSM-V criteria within the 3 months prior to the study, based on a clinical interview; 4) history of metabolic or other diseases known to affect the central nervous system (see (40) for similar criteria); 5) extensive metal dental hardware (e.g. braces and large metal dentures; fillings were acceptable) or other metal objects in the head, neck, or face areas that could cause artefacts in the MEG data, not removable during pre-processing; and 6) suicidal ideation as evaluated using the Beck Depression Inventory (BDI-II), i.e. any participant reporting a score of '2' or '3' on the BDI –II: item 9 (suicidal thoughts or wishes), confirmed in follow-up risk assessment.

All participants were allowed to be on their currently prescribed medications, but to remain on the same medication regimen as best they could during the course of the IASIS treatment. As listed in Table 1, two participants were taking an anti-depressant SSRI; they remained on the SSRI and kept the same dosage throughout IASIS treatment. The rest of the participants were not on any medications. Past history of drug and alcohol use were elicited in detail in the screening interview. Additionally, participants were asked to refrain from drinking alcohol or using illicit drugs the night before the MEG scan.

In the baseline interview, PCS in all participants with mTBI were assessed using the Rivermead Post-Concussion Symptom Questionnaire (RPCSQ) (41). This questionnaire contains 16 categories: 1) headaches; 2) feelings of dizziness; 3) nausea and/or vomiting; 4) noise sensitivity, easily upset by loud noise; 5) sleep disturbance; 6) fatigue, tiring more easily; 7) being irritable, easily angered; 8) feeling depressed or tearful; 9) feeling frustrated or impatient; 10) forgetfulness, poor memory; 11) poor concentration; 12) taking longer to think; 13) blurred vision; 14) light sensitivity, easily upset by bright light; 15) double vision; and 16) restlessness. The RPCSQ measures the extent to which a symptom is problematic, where 0 = not experienced, 1 = no more of a problem, 2 = mild problem, 3 = moderate problem, and 4 = severe problem. Only participants with persistent symptoms in at least three of the above categories during the baseline assessment were recruited into the study. After the IASIS treatment, the same RPCSQ was used to assess the post-treatment PCS in the participants with mTBI during a follow-up interview. One of the main study outcomes was the change in RPCSQ scores from pre- to post-IASIS treatment.

IASIS LIP-tES treatment procedure

IASIS (Micro Current Neurofeedback) programme used in this study is a 6-week (two 30-minute sessions per week) passive neurofeedback intervention with EEG monitoring. The IASIS device uses five EEG electrodes. The EEG interface device is the J&J Engineering I-330 C2, provided specifically for, and labelled for, IASIS, in accordance with specifications by Mind-Brain Training Institute. The software is IASIS 5.0, and it is supported by Physiolab 2007 supplied by J&J Engineering. The EEG sample frequency is 256 samples per second on each of two EEG acquisition channels.

The feedback LIP-tES is delivered via the four EEG leads (A+, A−, B+, B−), with respect to the Common Neck Reference (isolated). During each session, two electrodes (A − and B−) are attached to the participant's left and right mastoids, while the remaining two electrodes (A+ and B+) are moved to various locations on the scalp. All four (A+, A−, B+, B−) electrodes are involved in applying weak electric current pulses back to the brain (the feedback process). The feedback signal consists of two types of narrow pulses. Type-1 pulses are about 120 ns in duration, and 150 mV in amplitude in three Schedules (see Appendix 2). The repetition rate of the feedback pulse train is determined dynamically by adding the dominant brainwave (EEG) frequency, selected from the range of 2–12.5 Hz, to the frequency specified in each time interval of the three pre-programmed Schedules used in the study (see Appendix 2). The dominant frequency was acquired from the difference EEG signal between the A+ and A− electrodes using a trailing window Fast-Fourier Transform (FFT). Type-2 pulses are KHz carrier signals with frequency modulated upwards, creating a kind of 'chirp' pulses in which each pulse lasts about several milliseconds. These 'chirp' pulses were delivered as trains with 3.6 Hz fixed repetition rate, independent of the EEG signal.

Usually, the A+ and B+ electrodes are moved to various places during each treatment session. However, this step may disrupt the treatment and also draw unnecessary attention from the participant to specific electrode sites. In the present study, we prepped and pre-placed a set of electrodes on the scalp of the participant following the 10–20 EEG configuration. These 10–20 sites were the potential sites for the A+ and B+ electrodes. During the treatment sessions, the electrode inputs to the EEG interface device for the A+ and B+ electrodes (selected from the pre-placed 10–20 configuration) were switched, without the participant's knowledge, so that the participant could not tell which sites were activated. Out of

the standard 10–20 electrode sites, electrode pairs activated were: F3/F4, C3/C4, P3/P4, O1/O2, T5/T6, Fz/Pz, FPz/Cz, FP1/FP2, F9/F10, F9/FC3. Each Schedule takes between 22–25 seconds per site and each Schedule was delivered twice per electrode pair.

For the purpose of standardizing the research protocol, we focused on three different Schedules: Genesis, Balanced Energy, and Activation (see Appendix 2 for details of each Schedule). Genesis Schedule was performed during the first two visits. Balanced Energy Schedule was performed for the third and fourth visit. This Schedule provides a set of varied offset frequencies that change at 2-second intervals. Activation Schedule was performed for the eight remaining visits.

MEG and MRI data acquisition

Resting-state MEG data were collected using the VectorView™ whole-head MEG system (Elekta-Neuromag, Helsinki, Finland) with 306 MEG channels. For each participant, two 5-minute sessions with eyes closed were acquired. To co-register the MEG with the anatomical images of the participants, T1-weighted structural MRI of the participant's head was collected using a General Electric 1.5T Excite MRI scanner. The T1-weighted images were also used to extract the brain volume and innermost skull surface (SEGLAB software developed by Elekta/Neuromag). Realistic Boundary Element Method (BEM) head model was used for MEG forward calculation (42,43). Appendix 1 provides the technical details about the MEG and MRI data acquisitions and the MEG pre-processing procedures for removing artefacts.

Other conventional MRI sequences typical for identifying structural lesions in participants with TBI were also performed: 1) Axial T2*-weighted; 2) Axial fast spin-echo T2-weighted; and 3) Axial FLAIR. The conventional MRIs were carefully reviewed by a Board-certified neuroradiologist (R.R. Lee); no visible lesions were found on the MRI of any participant.

MEG source magnitude imaging using Fast-*VESTAL*

MEG source images were obtained using Fast-VESTAL method (44). In both five-minute rs-MEG data sessions with eyes closed, sensor-waveforms were run through a band-pass filter for 1–4 Hz (delta band). The data set was then divided into 2.5-second duration epochs, and sensor waveform covariance matrices were calculated for each epoch. A total sensor-waveform covariance matrix for the entire 10-minute recording was calculated by concatenating the covariance matrices from individual epochs. Using the total covariance matrix, voxel-wise MEG slow-wave source magnitude images that cover the whole brain were obtained for each participant following the Fast-VESTAL procedure (44). An Objective Pre-whitening Method was applied to remove correlated environmental noise and objectively select the dominant eigen-modes of sensor-waveform covariance matrix (44).

Fast-VESTAL has been successfully used to obtain comprehensive MEG source-magnitude images covering the entire brain for different frequency bands of resting-state brain rhythms (44). The second-order cone programming (SOCP) approach in the minimum L1-norm solver of the SeDuMi software (http://sedumi.ie.lehigh.edu/) was used in the present study. SOCP corrects orientation bias in a one-step approach (45,46). The technical details of Fast-VESTAL using the SOCP formulation is in the appendix of (47).

Characterizing abnormal MEG slow-wave source imaging in individual participants with mTBI

The procedure for detecting abnormal MEG slow-wave in single subjects using a voxel-wise approach is detailed in previous study (27). In the present study, MEG slow-waves in single subjects were evaluated against our voxel-wise normative database that contains 96 healthy individuals between the ages of 18 and 55. The normative database is in MNI-152 atlas coordinates for the MEG source magnitude (spatially smoothed and logarithm transformed). After spatial smoothing and logarithm transformation, the MEG source magnitude images from each participant with mTBI were registered to the MNI-152 coordinates, and then converted into Z-score maps using the voxel-wise normative database (27). The abnormal MEG slow-wave generation from each participant with mTBI was characterized by the voxels in the Z-score maps with statistical significance (q-value <0.01) after controlling the family-wise error due to multiple comparisons using false discovery rate approach (48). We also calculated total abnormal MEG Z-scores by summing up the Z-score from all voxels that showed statistically significant slow-wave generation. The focus of our analyses was on the pre- and post-IASIS change in the abnormal MEG slow-wave generation for both voxel-wise Z-score maps and the total abnormal MEG Z-scores.

Results

Pre- and post-IASIS changes in PCS scores

A key element of the present study was to examine changes in clinical symptoms after IASIS treatment. We found that clinical symptoms were significantly reduced in the six individuals with mTBI who participated in the IASIS treatment. Table 2 lists the RPCSQ scores from the pre- and post-IASIS assessments in each participant. PCS total scores across 16 categories were markedly reduced after the IASIS treatment in all participants (Table 2, bottom row; Figure 1A), and the effect sizes associated with the treatment effects were all very large (Cohen's $d > 1.0$). The individuals with mTBI showed a marked reduction of 52.76% ± 26.4% in PCS total score. The observed reduction in PCS total scores between the pre- and post-IASIS assessments was statistically significant (paired group t-test, $t = 5.80$, $p < 0.01$, Cohen's $d = 2.37$). Sleep Disturbances, a sub-category of the RPCSQ, also were significantly reduced post-IASIS treatment (paired group t-test, $t = 3.00$, $p < 0.05$, Cohen's $d = 1.22$).

Pre- and post-IASIS changes in total abnormal Z-scores from MEG slow-wave imaging

Figure 1B shows a striking reduction in the total abnormal Z-scores that measured the abnormal MEG slow-wave

Table 2. Rivermead post-concussion symptom scores from pre- and post-IASIS assessments in six participants with mTBI.

	Participant #1		Participant #2		Participant #3		Participant #4		Participant #5		Participant #6	
Rivermead PCS Questionnaire	Pre-	Post-	Pre-	Post-	Pre-	Post-	Pre-	Post-	Pre-	Post-	Pre-	Post-
Headaches	3	1	4	3	4	1	0	0	4	4	3	1
Feelings of Dizziness	3	2	4	2	0	0	0	0	3	3	1	0
Nausea and/or Vomiting	2	1	4	0	0	0	0	0	3	3	0	0
Noise Sensitivity, Easily Upset by Loud Noise	2	2	4	1	2	1	2	1	4	4	4	1
Sleep Disturbance	4	2	4	1	0	0	2	0	3	3	3	1
Fatigue, Tiring More Easily	2	1	0	0	2	0	0	0	3	2	2	1
Being Irritable, Easily Angered	3	1	4	1	2	1	1	0	4	4	3	1
Feeling Depressed or Tearful	2	1	4	3	0	0	1	0	3	3	0	0
Feeling Frustrated or Impatient	4	2	4	3	3	1	1	0	4	3	2	1
Forgetfulness, Poor Memory	4	1	4	2	4	3	2	0	3	3	4	1
Poor Concentration	4	1	4	3	4	3	2	0	3	3	2	1
Taking Longer to Think	3	1	4	3	4	3	2	0	3	3	3	1
Blurred Vision	2	2	3	3	0	0	0	0	3	0	1	0
Light Sensitivity, Easily Upset by Bright Light	2	2	4	1	4	2	0	0	4	4	2	1
Double Vision	2	2	3	1	0	0	0	0	1	0	0	0
Restlessness	4	3	0	0	2	0	1	0	3	3	1	1
TOTAL	46	25	54	27	31	15	14	1	51	45	31	11

Scores on the RPCSQ range from 0 to 4 for individual symptoms where 0 = not experienced, 1 = no more of a problem, 2 = mild problem, 3 = moderate problem, and 4 = severe problem. *Participant #5 did not complete the scheduled protocol: He did only four sessions.

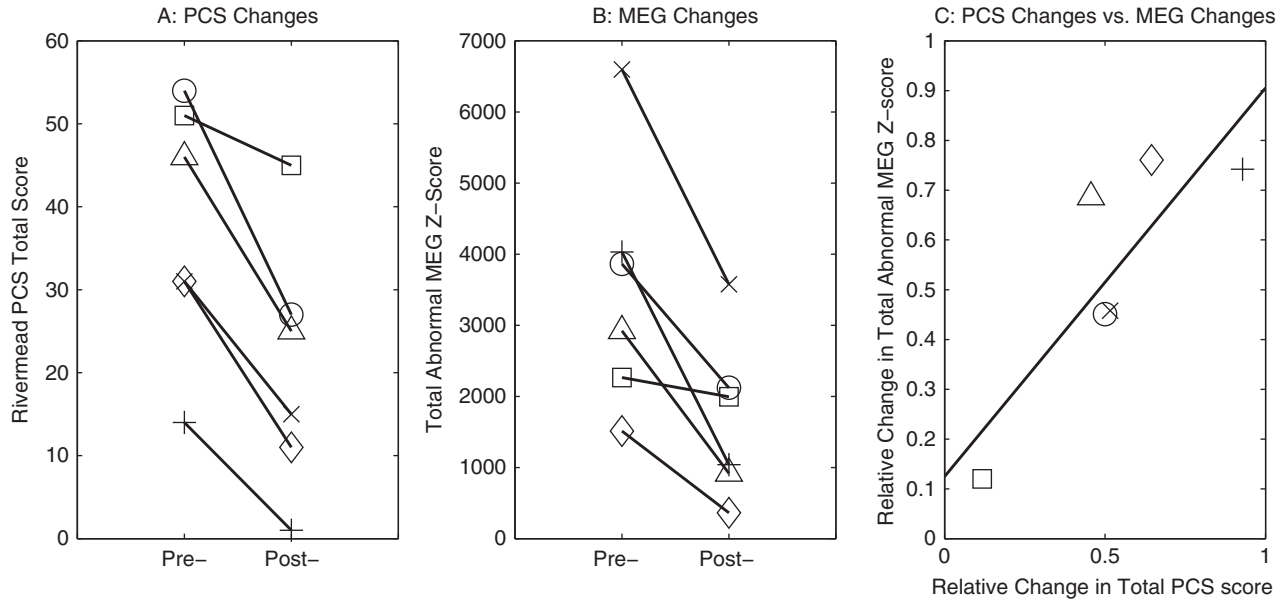

Figure 1. A: Significant reduction in total Rivermead PCS scores between pre- and post-IASIS assessments ($p < 0.01$). B: Significant reduction in total abnormal Z-score MEG slow-wave source imaging between pre- and post-IASIS MEG exams ($p < 0.01$). C: Relative change in total abnormal MEG Z-score correlates with relative change in total PCS score ($p < 0.05$). Symbols 'Δ', 'O', '×', '+', '□', and '◊' represent Participants #1, #2, …, and #6, respectively.

generation between the pre- and post-IASIS MEG exams, with an average reduction of 53.6% ± 24.6% in total abnormal MEG slow-wave Z-score. The change in total abnormal MEG Z-scores was also statistically significant (paired group t-test, $t = 4.28$, $p < 0.01$, Cohen's $d = 1.75$).

Next, we correlated the change in MEG slow-waves due to treatment with change in the total PCS scores. In this analysis, we examined two measures: 1) the absolute change of both total abnormal MEG Z-scores and the PCS scores, i.e. pre-post; and 2) the relative change for both total abnormal Z-scores from MEG slow-wave imaging and the PCS scores calculated according to the following formula: (pre-post)/pre. The results showed no significant correlation between absolute change of total abnormal MEG Z-scores and the PCS scores ($r = 0.23$, $p = 0.65$). However, *relative* total abnormal MEG Z-score change significantly correlated with *relative* total PCS score change. Figure 1C showed a significant positive correlation between the relative total abnormal MEG Z-score change and relative total PCS score change ($r = 0.84$, $p < 0.05$).

Pre- and post-IASIS changes in both PCS and MEG slow-wave imaging for individual participants

In this subsection, detailed information is provided for each participant about pre- and post-IASIS changes related to PCS and abnormal voxel-wise MEG slow-waves. Table 2 lists the RPCSQ scores in each category from the pre- and post-IASIS assessments in each participant. Figure 2 shows the voxel-wise MEG findings for assessing the effect of IASIS treatment on brain functioning in all six participants with mTBI.

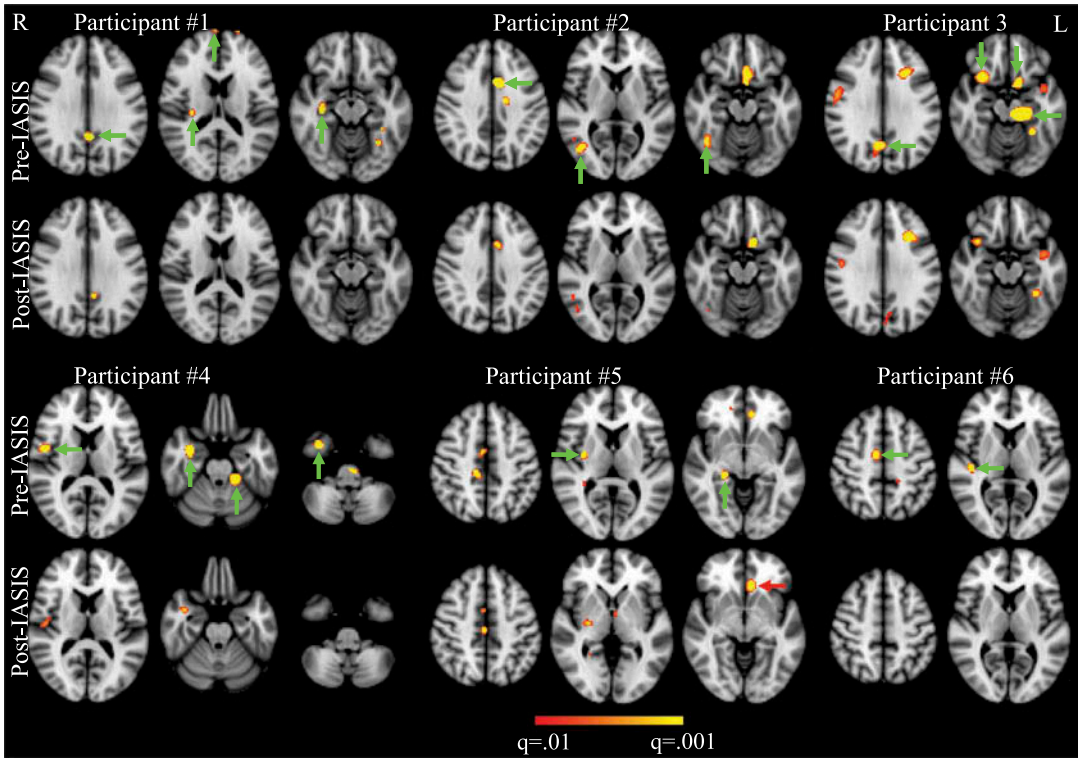

Figure 2. Changes in abnormal MEG slow-waves between pre- and post-IASIS MEG exams in six participants with mTBI. Green arrows indicate areas with abnormal slow-waves at the baseline but markedly reduced (>30%) after IASIS. Red arrow indicates an area with markedly increased (>30%) slow-wave after IASIS in Participant #5, who completed only 4 of 12 scheduled sessions. The hot spots without arrows indicate abnormal slow waves that did not show marked change (<30%) after IASIS treatment.

Representative axial slices with major abnormal slow-waves ($q < 0.01$, FDR correction) are plotted in Figure 2.

Participant #1 was a Marine who experienced an mTBI due to a mortar blast. During and following the IASIS treatment, he reported that his symptoms greatly abated, going from severe to no problem or mild. His overall RPCSQ score went from 46 to 25, a reduction of 45.7%. He also mentioned that he had completely discontinued his use of nicotine after the IASIS treatments, which he claimed was a beneficial result of the treatments. At 6 months after IASIS, he stated that the treatment effects had persisted and that he still did not use nicotine.

Compared with pre-IASIS MEG, his post-IASIS MEG showed marked reduction of 68.6% in total abnormal MEG Z-score (Figures 1B and 1C). Abnormal slow-waves were markedly reduced from frontal pole, posterior cingulate cortex (PCC), right insula, and right hippocampus (Figure 2). In studies of headaches and migraine, activation of the insula, which is a component of the 'pain matrix', is attributed to the processing of pain and unpleasantness (49–52). The PCC is also a part of the pain matrix (49,51). Following treatment, his headaches were reduced, as were slow-waves in both the insula and the PCC. The MEG findings were also compatible with reduced PCS for memory function (related to hippocampus) (32).

Participant #2 was involved in a multi-vehicle accident that resulted in a loss of consciousness, which led to mTBI with widespread moderate to severe symptoms. Halfway through the IASIS sessions, she reported a reduction in stuttering, anxiety, headaches, and less visual and auditory overstimulation (particularly reduction of photophobia). After the completion of all IASIS treatments, she reported an even greater reduction of symptoms (i.e. by 50.0%). Her overall score for RPCSQ went from 54 to 27.

Her total abnormal MEG Z-score post-IASIS was markedly reduced by 45.1% relative to the baseline MEG exam (Figures 1B and 1C). Specifically, markedly reduced MEG slow-waves after treatment were found in anterior cingulate cortex (ACC), and right occipital areas, including the right lateral occipital cortex and right occipital fusiform gyrus spanning the lingual gyrus (Figure 2). Reduced slow-waves in the ACC, which is also part of the pain matrix (49–52), was compatible with her reduced headaches following treatment. Additionally, her reduced slow-waves after treatment in the right fusiform gyrus and lingual gyrus were compatible with the decrease in photophobia, a symptom that is linked with the lingual gyrus, a visual processing area (53).

Participant #3 was involved in a car accident. After IASIS, his symptoms drastically reduced by 51.6% from an initial RPCSQ total score of 31–15. Light sensitivity was reported as only mild whereas headaches, noise sensitivity, irritability, and frustration no longer a problem. Importantly, initially severe symptoms were more moderate after treatment (i.e. forgetfulness/poor memory, poor concentration, and taking longer to think).

Compared with the pre-IASIS exam, his post-IASIS total abnormal MEG Z-scores decreased by 45.8% (Figures 1B and 1C). Specifically, striking decreases in abnormal slow-waves

were notable in the PCC, bilateral OFC, and left hippocampus (Figure 2). The MEG findings are compatible with reduced PCS for memory problems (hippocampus) (32) and headaches (PCC) (49,51).

Participant #4 was an Army soldier who experienced an IED blast while riding in an Mine-Resistant Ambush Protected vehicle. After three visits and throughout the remaining IASIS sessions, he reported that his quality of sleep had improved, leaving him well rested with a positive change in attitude. Upon finishing all IASIS sessions, he recorded an overall score of 1 on the RPCSQ, a reduction of 92.9% in total RPCSQ score. He noted that noise sensitivity was no more of a problem for him. All other symptoms were listed as absent, which meant that he was essentially symptom-free.

The pre- and post-IASIS MEG exams show that the total abnormal MEG Z-scores were reduced by 74.2% (Figures 1B and 1C). Reductions of abnormal slow-waves were striking in the right inferior-lateral parietal area and superior temporal gyrus/auditory cortex, right hippocampus and amygdala, right inferior temporal pole, and left cerebellum (Figure 2). Changes in the central auditory system may play an important role in hyperacusis, an intolerance of normal environmental sound (54). Following treatment, he had less noise sensitivity, consistent with the observed reduction of slow-waves in the superior temporal gyrus/auditory cortex. Additionally, MEG findings were compatible with reduced PCS for memory loss (hippocampus) (32).

Participant #5 was a Marine who experienced blunt head trauma when a piece of furniture struck his head. He experienced another blunt head trauma when a chair that he was sitting broke, intensifying his previous symptoms. He only finished 4 out of the 12 required IASIS treatment sessions. From the beginning, he missed or rescheduled multiple sessions. Because it appeared likely that he might not (actually he did not) finish his IASIS treatment, an MEG exam was performed following his fourth visit, and that MEG was used for this paper. After his fourth IASIS visit, there was a 11.8% reduction in total RPSCQ symptoms (51 in pre-IASIS exam to 45 after the fourth session), which was not nearly as remarkable as that of individuals who completed all sessions.

The pre-IASIS MEG exams show that he had abnormal slow-wave generation from right ACC and PCC, right striatum/insular cortex, right parahippocampus, and left ventromedial prefrontal cortex (vmPFC) (Figure 2). Following the fourth IASIS treatment visit, his total abnormal MEG Z-score showed only a marginal reduction of 12.0% (Figures 1B and 1C). Specifically, his abnormal slow-wave generation from the right ACC and PCC remained essentially the same. Reduced slow-waves were observed from his right striatum/insular cortex and his right parahippocampus, but *increased* slow-wave generation was found from his left vmPFC (Figure 2). The MEG findings were compatible with his persistent and ongoing PCS at his fourth visit for headache (ACC and PCC) (49–52). Dysfunction in vmPFC can impair modulation of emotional reactions, resulting in increasing irritability and impairing decision making (55), which was consistent with his severe symptom of irritability.

Participant #6 was an Army soldier who experienced a blast due to an IED while riding in a Humvee. Throughout the IASIS sessions, he noted improvement with sleep quality, accompanied by feeling more energetic. By the end of the sessions, his symptoms were all scored as no more of a problem. The total RPCSQ score reduced by 64.5%.

After treatment, his total abnormal MEG Z-scores decreased by 76.1% (Figures 1B and 1C). Notable decreases in abnormal slow-wave generation were observed from the right auditory cortex and the right supplementary motor area (SMA) and ACC (Figure 2). The SMA is also a component of the pain matrix (49). Following treatment, the abatement of his headaches was compatible with reduced slowing in both the SMA and the ACC (49–52). The MEG findings were also compatible with reduced PCS for noise sensitivity (auditory cortex in the superior temporal gyrus) (54).

Discussion

Consistency with previous LIP-tES studies

Our findings that IASIS treatment significantly reduced PCS in participants with mTBI are consistent with TBI studies that used other types of LIP-tES treatment techniques, such as FNS (19–23). The present study also found significantly reduced abnormal MEG slow-wave generation in individuals with mTBI after IASIS. Our finding is compatible with the study by Larsen and colleagues that reported significant decreases in EEG amplitude at the highest amplitude electrode site and at electrode Cz in a mixed population of individuals with TBI and other neurological and/or psychological disorders (20). However, our study demonstrates reduction in abnormal slow-wave generation along with improved PCS after IASIS treatment in individuals with mTBI and documented PCS. Larsen and colleagues also did not specify the range of frequency or frequency band(s) that were altered by LIP-tES treatment. In contrast, our results were directly linked to abnormal MEG slow-waves in delta frequency band (1–4 Hz), which is firmly grounded in neurophysiological studies in animals (33–35) and subsequently in humans (25–30). Larsen and colleagues' results were also based on analyses in sensor space outside the brain (i.e. EEG electrode positions), whereas our MEG source imaging findings were in image space, inside the brain, and specific to different brain areas. Since an EEG electrode may pick up the signals from multiple brain areas, the signal from one abnormal brain source may contribute to multiple EEG electrodes. By solving the MEG inverse source imaging problem using Fast-VESTAL (27,44), our study is truly a neuroimaging study. In particular, our MEG source imaging approach provides direct measures in the brain regarding the changes of abnormal MEG slow-wave signals following the IASIS treatment (see Figure 2).

The healing mechanism of slow-waves after neuronal injury

Abnormal rs-MEG slow-wave during wakefulness can be used as an imaging marker for sensitive detection of neuronal injury in mTBI (25–31). A more fundamental question is

whether slow-wave generation is merely a negative consequence of neuronal injury or a signature of ongoing neuronal rearrangement/healing that occurs at the site of the injury. These two different views will lead to opposing mTBI treatment strategy designs. If the abnormal slow-wave generation is a negative consequence of the injury, the strategy should focus on cancelling the slow-waves during the treatment. On the other hand, if the slow-wave generation is part of a process of neuronal healing, the treatment should focus on potentiating endogenous slow-wave generation during the treatment. The literature on neural plasticity and stroke recovery supports the healing mechanism hypothesis of slow-waves (56,57). Of course, for a successful treatment strategy, a desirable outcome should always be the ultimate elimination/substantial reduction of the abnormal slow-waves in mTBI *by the end of the treatment course*.

We favour the neuronal healing mechanism of slow-waves in mTBI. It has been shown that long-term potentiation induced in the motor cortex in humans, by means of intermittent theta burst stimulation, is accompanied by a large and enduring increase of delta waves during wakefulness, suggesting a prominent role of delta waves in the neural plasticity processes taking place during the awake state (56). Accordingly, the delta waves could be an epiphenomenon of ongoing cortical plasticity during wakefulness as during sleep and of the attempt of the cortex to re-establish a near-physiological functioning (56). Furthermore, it was recently shown in an animal TBI study in rodents with diffuse axonal injury, that enhancing slow-wave sleep acutely after trauma by sleep modulation may have a beneficial disease-modifying effect in animals with TBI. The authors suggested that slow-waves in the delta-frequency range could be the key to functional improvement after TBI (58). The mechanism of slow-wave-potentiated improvement could be linked with enhanced clearance of proteins and other waste products from interstitial space in brain (58). Slow-wave sleep and anaesthesia were associated with enhanced clearance of potentially neurotoxic waste products (e.g. β-amyloid) in adult mice (59), whereas a correlation between β-amyloid accumulation and disruption of non-REM sleep was observed in Alzheimer's disease patients (60), further supporting the potential benefits of enhanced slow-wave activity in treatment for TBI (58).

Exploring the neural mechanism of IASIS for mTBI treatment

The neural mechanisms underlying IASIS, and LIP-tES in general, are not completely understood (16). LIP-tES belongs to a large category of transcranial electrical stimulation (tES) techniques that includes transcranial direct current stimulation (tDCS), transcranial alternating current stimulation (tACS), and transcranial random noise stimulation (tRNS) (61–63). It has been proposed that anodal tDCS and tRNS increase neuronal excitability and may consequently enhance behavioural performance, that cathodal tDCS decreases neuronal excitability and subsequently worsens behavioural performance, and tACS increases neuronal excitability via entrainment of the desired neuronal firing frequency and consequently modulates performance (64). However, this simplistic, sliding-scale reasoning (from excitation to inhibition or vice versa) does not always explain the results at either the neurophysiological or the behavioural level (63). Other models of tES mechanisms include the Stimulation-Dependent, Activity-Dependent, Network Activity-Dependent, Excitation-Inhibition Balance, and Zero-Sum Models, each with its own strengths and limitations (see review in (63)).

Recently, Fertonani and Miniussi proposed stochastic resonance (SR) as a useful mechanism to explain the general neuromodulation effects of tES (63). SR is a phenomenon wherein an endogenous oscillatory brain signal that is normally too weak to be detected can be boosted by adding to the signal some noise or input, which contains a wide spectrum of frequencies. We believe that the SR model may explain the treatment effects of LIP-tES, including IASIS, for mTBI. In IASIS, when the repetition rate of the low-intensity pulses is similar to an underlying endogenous oscillatory brain signal, the SR effect may occur. Between the nanosecond-duration Type-1 and millisecond-duration Type-2 pulses in IASIS, we believe that Type-2 pulses with repetition rate of 3.6 Hz are the more likely ones to potentiate underlying endogenous slow-waves brain rhythms. This is because the duration of pulses needs to be sufficiently long (i.e. in the scale of ms) to influence the neurotransmitters at the synapses (all with time constants in the ms range or longer) (32). Type-1 pulses with nanosecond duration are probably too short to have a significant impact on the neurotransmitters, thus they are unlikely to play significant role in potentiating underlying endogenous slow-waves brain rhythms. Therefore, we believe that by potentiating endogenous slow-wave generation with Type-2 pulses during the treatment sessions, IASIS enhances the healing process underlying the sites of the injury. Consequently, IASIS treatment ultimately eliminates /substantially reduces the abnormal slow-waves in mTBI by the end of the treatment course when the healing is accomplished. We are exploring this idea further by studying rs-MEG exams right before, and immediately after an IASIS treatment session. So far, the preliminary result supports the idea that IASIS potentiates endogenous slow-wave generation immediately after a treatment session (Huang et al., in preparation).

Absolute versus relative changes in MEG and PCS scores

Although we found no significant correlation between absolute change in total abnormal MEG Z-scores and total PCS scores, *relative* change in the total abnormal MEG Z-score was significantly correlated with *relative* change in the total PCS score of the participants with mTBI (Figure 1C). We believe the lack of a significant correlation between the absolute change in MEG and PCS measures was partly due to inter-subject variability in participants' criteria for rating the severity of their symptoms. One participant's internal standard for rating the existence and severity of the PCS may be different from that of another participant. Hence, the symptom rating process is subjective to the participant's internal standard. However, as long as such an internal standard remained the same between the baseline and post-IASIS assessments, the relative change scores (i.e. absolute change normalized by the

score in the baseline) should be less subjective. Furthermore, the same difference score in PCS (post-treatment versus pre-treatment) without normalization could have different meanings in one participant with a more liberal standard to rate his/her PCS versus another participant who applies a more conservative rating standard. A participant with a high PCS score at baseline would have 'more room' to improve than another subject with a low PCS score at baseline. For example, for a participant who had a total PCS score of 60 at baseline, with a reduction of 20 points after the treatment, he/she would still have substantial remaining PCS with a total score of 40 after the treatment. However, for another participant who had a total PCS score of 20 at baseline, with a reduction of 20 points, he/she would fall in the symptom-free range after the treatment. The main reason in our approach of using a normalized difference score was to remove such biases.

A similar argument would apply to the MEG Z-scores. Furthermore, the MEG slow-wave generation may be affected by medications that our participants were taking. We did not require the participants to temporarily stop their normal medications. The main advantage of allowing the participants to remain on their medications was to minimize the interruption to their daily life and hence, minimize study attrition. However, some medications may modify MEG slow-wave activity. In particular, neuroleptic sedatives, antidepressants, and hypnotics can globally change brain activity (65). Thus, an advantage of using relative change in MEG total abnormal Z-scores as a measure of treatment outcome is that it should reduce the effects that medications may have on slow-wave activity. Hence, the association between relative changes in MEG abnormal slow-wave activity and relative change in PCS after IASIS in mTBI should not be seriously confounded by medications.

Duration of IASIS treatment

The typical duration of IASIS treatment is 10 weeks (two 30-minute sessions per week) which is based on previous experience from participants with a variety of neurological and/or psychological disorders. Due to study participant availability and resource constraints, we utilized a 6-week, two session per week intervention programme in the present mTBI study. Noting that Participant #5 only finished 4 out of the 12 treatment sessions and he only showed marginal reductions in PCS and MEG slow-waves. This example shows that dropping off early from the treatment programme is not good. On the other hand, prolonging the treatment beyond the necessary duration may not be beneficial for the participant either. Future research is needed to examine the optimal treatment duration of IASIS for mTBI.

Limitations of the study and suggestions for future studies

There are several limitations to the present pilot study. First, the effects of IASIS treatments on neurobehavioural outcomes need to be evaluated using larger mTBI samples. However, despite our small sample size, statistical analyses of pre-post treatment showed very large effect sizes suggesting that IASIS treatments are promising for reducing PCS and the generation of abnormal slow waves. Second, future studies using blind and double-blind designs with a sham group are needed to better validate the efficacy of IASIS and more generally, LIP-tES, for treating mTBI. Third, since all participants in the present study were on their standard medical regimens and taking their normal medications, we do not consider this to be a limitation of the study. Nevertheless, studying a group of individuals with mTBI who are medication-free or for whom their medication is temporarily withheld would completely remove this confound. However, such a group does not reflect the typical mTBI population and may be extremely difficult to recruit. Fourth, the sites for delivering LIP-tES current in the present study were predetermined by the three standard protocols: no spatial information from MEG slow-wave loci was used to guide the treatment. Future study with guidance from MEG slow-wave source imaging may provide customized protocols for each participant with mTBI to optimize the treatment effect. Lastly, our individual-subject analyses pertaining to possible associations between treatment-related improvements in specific symptoms and regional reductions in abnormal slow-wave generation are qualitative and speculative, owing to the small mTBI sample. Larger samples will be required to quantitatively link regional changes in slow-wave activity with changes in specific PCS in mTBI.

Despite these limitations, we do not believe that the significant reductions (i.e. over 50% on average) of PCS and abnormal MEG slow-waves can be explained by potential placebo effect. Although some sub-categories of the self-reported RPCSQ may be sensitive to placebo, the Sleep Disturbance sub-category of the RPCSQ is typically related to the number of hours in sleep and quality of sleep which are usually more objective and less sensitive to placebo effect. Thus, in our participants with mTBI, the significant reduction in the Sleep Disturbance sub-category of the RPCSQ makes it unlikely to be a placebo effect. Furthermore, the rs-MEG exam is task-free, without any influence of performance variables, and more objective than the behavioural measures. The significant reduction of MEG slow-waves in our participants with mTBI makes placebo effect an unlikely explanation to our MEG findings. Of course, future research with a larger sample, a sham group, and with a blind or double-blind design will fully address the placebo effect. Next, we do not believe that a spontaneous mTBI recovery can explain such significant reductions in PCS and MEG slow-waves either. This is because all participants had a chronic mTBI with persistent PCS for an average of 48.2 (± 25.2) months ranging between 14 and 84 months, which substantially exceeded the acute and sub-acute phases of mTBI where spontaneous recovery is evident. Thus, it was unlikely that spontaneous mTBI recovery played any significant role during such a chronic phase of the disorder in this study.

Summary and conclusions

The present pilot study revealed for the first time neuroimaging-based evidence for functional changes in the brain that underlie LIP-tES treatment effects in individuals with mTBI. Abnormal MEG slow-waves were significantly reduced after IASIS treatments in approximately the same

brain areas that showed abnormal slow-wave generation during the baseline (pre-treatment) MEG exam. Importantly, PCS were also typically reduced, or even eliminated altogether, following IASIS treatments. Furthermore, relative reductions of MEG slow-wave total abnormal Z-score correlated with the relative reduction of the PCS score. The information regarding loci that generate abnormal MEG slow waves in each individual with mTBI may also be used as a guide in developing an optimal and subject-specific IASIS treatment plan for that individual. Altogether, the present study sets the stage for a new avenue of research that can advance an understanding of the mechanisms underlying low-intensity transcranial stimulation and its relevance to behavioural outcomes that significantly impact the quality of life in individuals with mTBI.

Declaration of Interest

This work was supported in part by Merit Review Grants from the US Department of Veterans Affairs (PI: M.X. Huang, I01-CX000499, I01-RX001988, MHBA-010-14F, NURC-022-10F, NEUC-044-06S)

Although Mr Barry Bruder and Mr Corey Snook are associated with IASIS Technologies, Inc., and Mind-Brain Training Institute, respectively, their contributions to this work was limited to providing to the UCSD group training, technical support, and technical information related to the IASIS system. Neither of them was involved in recruiting participants, data acquisition, or data analysis in the present study.

References

1. Centers for Disease Control and Prevention, and National Center for Injury Prevention and Control. Report to Congress on mild traumatic brain injury in the United States: steps to prevent a serious public health problem. Atlanta (GA, USA), 2003: Centers for Disease Control and Prevention.
2. MacGregor AJ, Dougherty AL, Galarneau MR. Injury-specific correlates of combat-related traumatic brain injury in operation Iraqi freedom. J Head Trauma Rehabil. 2011;26:312–18. 10.1097/HTR.0b013e3181e94404.
3. Bigler ED. Neuropsychology and clinical neuroscience of persistent post-concussive syndrome. J Int Neuropsychol Soc. 2008;14:1–22. 10.1017/S135561770808017X.
4. Alexander MP. Mild traumatic brain injury: pathophysiology, natural history, and clinical management. Neurology. 1995;45:1253–60. 10.1212/WNL.45.7.1253.
5. Binder LM. A review of mild head trauma. Part II: clinical implications. J Clin Exp Neuropsychol. 1997;19:432–57. 10.1080/01688639708403871.
6. Binder LM. Persisting symptoms after mild head injury: a review of the postconcussive syndrome. J Clin Exp Neuropsychol. 1986;8:323–46. 10.1080/01688638608401325.
7. Bohnen N, Jolles J, Twijnstra A. Neuropsychological deficits in patients with persistent symptoms six months after mild head injury. Neurosurgery. 1992;30:692–95.
8. McCauley SR, Wilde EA, Miller ER, Frisby ML, Garza HM, Varghese R, Levin HS, Robertson CS, McCarthy JJ. Preinjury resilience and mood as predictors of early outcome following mild traumatic brain injury. J Neurotrauma. 2013;30:642–52. 10.1089/neu.2012.2393.
9. Rimel RW, Giordani B, Barth JT, Boll TJ, Jane JA. Disability caused by minor head injury. Neurosurgery. 1981;9:221–28.
10. Rutherford WH. Postconcussion symptoms: relationship to acute neurological indices, individual differences, and circumstances of injury. In: Levin H, Eisenberg H, Benton AL, eds. Mild head injury. New York: Oxford University Press, 1989;217–28.
11. Cooper DB, Bunner AE, Kennedy JE, Balldin V, Tate DF, Eapen BC, Jaramillo CA. Treatment of persistent post-concussive symptoms after mild traumatic brain injury: a systematic review of cognitive rehabilitation and behavioral health interventions in military service members and veterans. Brain Imaging Behav. 2015;9:403–20. 10.1007/s11682-015-9440-2.
12. Schneiderman AI, Braver ER, Kang HK. Understanding sequelae of injury mechanisms and mild traumatic brain injury incurred during the conflicts in Iraq and Afghanistan: persistent postconcussive symptoms and posttraumatic stress disorder. Am J Epidemiol. 2008;167:1446–52. 10.1093/aje/kwn068.
13. Terrio H, Brenner LA, Ivins BJ, Cho JM, Helmick K, Schwab K, Scally K, Bretthauer R, Warden D. Traumatic brain injury screening: preliminary findings in a US Army brigade combat team. J Head Trauma Rehabil. 2009;24:14–23. 10.1097/HTR.0b013e31819581d8.
14. Morissette SB, Woodward M, Kimbrel NA, Meyer EC, Kruse MI, Dolan S, Gulliver SB. Deployment-related TBI, persistent postconcussive symptoms, PTSD, and depression in OEF/OIF veterans. Rehabil Psychol. 2011;56:340–50. 10.1037/a0025462.
15. Jeter CB, Hergenroeder GW, Hylin MJ, Redell JB, Moore AN, Dash PK. Biomarkers for the diagnosis and prognosis of mild traumatic brain injury/concussion. J Neurotrauma. 2013;30:657–70. 10.1089/neu.2012.2439.
16. Ochs L. The Low Energy Neurofeedback System (LENS): theory, background, and introduction. J Neurotherapy. 2006;10:5–39. 10.1300/J184v10n02_02.
17. Ochs L. Flexyx neurotherapy system operating manual for the J&J USE2 and LLC. Walnut Creek, CA, USA: Flexyx,the I–330 ompact 2C EEG.1997.
18. Snook C, assignee. US patent application for "Method and system for retraining brainwave patterns using ultra low power direct electrical stimulation feedback" (Application #20140330157). 2013. http://patents.justia.com/patent/20140330157.
19. Nelson DV, Esty ML. Neurotherapy of traumatic brain injury/post-traumatic stress symptoms in Vietnam veterans. Mil Med. 2015;180:e1111–1114. 10.7205/MILMED-D-14-00696.
20. Larsen S, Harrington K, Hicks S. The LENS (Low energy neurofeedback system): a clinical outcomes study on one hundred patients at stone mountain center, New York. J Neurotherapy. 2006;10:69–78. 10.1300/J184v10n02_06.
21. Nelson DV, Esty ML. Neurotherapy for chronic headache following traumatic brain injury. Mil Med Res. 2015;2:22. 10.1186/s40779-015-0049-y.
22. Nelson DV, Esty ML. Neurotherapy of traumatic brain injury/posttraumatic stress symptoms in OEF/OIF veterans. J Neuropsychiatry Clin Neurosci. 2012;24:237–40. 10.1176/appi.neuropsych.11020041.
23. Schoenberger NE, Shif SC, Esty ML, Ochs L, Matheis RJ. Flexyx neurotherapy system in the treatment of traumatic brain injury: an initial evaluation. J Head Trauma Rehabil. 2001;16:260–74. 10.1097/00001199-200106000-00005.
24. Leahy RM, Mosher JC, Spencer ME, Huang MX, Lewine JD. A study of dipole localization accuracy for MEG and EEG using a human skull phantom. Electroencephalogr Clin Neurophysiol. 1998;107:159–73. 10.1016/S0013-4694(98)00057-1.
25. Huang MX, Theilmann RJ, Robb A, Angeles A, Nichols S, Drake A, D'Andrea J, Levy M, Holland M, Song T, et al. Integrated imaging approach with MEG and DTI to detect mild traumatic brain injury in military and civilian patients. J Neurotrauma. 2009;26:1213–26. 10.1089/neu.2008.0672.
26. Huang M-X, Nichols S, Robb A, Angeles A, Drake A, Holland M, Asmussen S, D'Andrea J, Chun W, Levy M, et al. An automatic MEG low-frequency source imaging approach for detecting injuries in mild and moderate TBI patients with blast and non-blast causes. Neuroimage. 2012;61:1067–82. 10.1016/j.neuroimage.2012.04.029.
27. Huang M-X, Nichols S, Baker DG, Robb A, Angeles A, Yurgil KA, Drake A, Levy M, Song T, McLay R, et al. Single-subject-based whole-brain MEG slow-wave imaging approach for detecting

abnormality in patients with mild traumatic brain injury. Neuroimage Clin. 2014;5:109–19. 10.1016/j.nicl.2014.06.004.
28. Huang M, Risling M, Baker DG. The role of biomarkers and MEG-based imaging markers in the diagnosis of post-traumatic stress disorder and blast-induced mild traumatic brain injury. Psychoneuroendocrinology. 2016;63:398–409. 10.1016/j.psyneuen.2015.02.008.
29. Lewine JD, Davis JT, Sloan JH, Kodituwakku PW, Orrison WW Jr. Neuromagnetic assessment of pathophysiologic brain activity induced by minor head trauma. AJNR Am J Neuroradiol. 1999;20:857–66.
30. Lewine JD, Davis JT, Bigler ED, Thoma R, Hill D, Funke M, Sloan JH, Hall S, Orrison WW. Objective documentation of traumatic brain injury subsequent to mild head trauma: multimodal brain imaging with MEG, SPECT, and MRI. J Head Trauma Rehabil. 2007;22:141–55. 10.1097/01.HTR.0000271115.29954.27.
31. Robb Swan A, Nichols S, Drake A, Angeles A, Diwakar M, Song T, Lee RR, Huang M-X. Magnetoencephalography slow-wave detection in patients with mild traumatic brain injury and ongoing symptoms correlated with long-term neuropsychological outcome. J Neurotrauma. 2015;32:1510–21. 10.1089/neu.2014.3654.
32. Kandel ER, Schwartz JH, Jessell TM, Siegelbaum SA, Hudspeth AJ. Principles of neural science. 5th. New York: McGraw-Hill Companies, 2013, Inc.
33. Gloor P, Ball G, Schaul N. Brain lesions that produce delta waves in the EEG. Neurology. 1977;27:326–33. 10.1212/WNL.27.4.326.
34. Ball GJ, Gloor P, Schaul N. The cortical electromicrophysiology of pathological delta waves in the electroencephalogram of cats. Electroencephalogr Clin Neurophysiol. 1977;43:346–61. 10.1016/0013-4694(77)90258-9.
35. Schaul N, Gloor P, Ball G, Gotman J. The electromicrophysiology of delta waves induced by systemic atropine. Brain Res. 1978;143:475–86. 10.1016/0006-8993(78)90358-X.
36. Schaul N. The fundamental neural mechanisms of electroencephalography. Electroencephalogr Clin Neurophysiol. 1998;106:101–07. 10.1016/S0013-4694(97)00111-9.
37. McCarley RW, Massaquoi SG. A limit cycle mathematical model of the REM sleep oscillator system. Am J Physiol. 1986;251:R1011–1029.
38. The Management of Concussion/mTBI Working Group. VA/DoD clinical practice guideline for management of concussion/mild traumatic brain injury. J Rehabil Res Dev. 2009;46:CP1–68. 10.1682/JRRD.2008.03.0038.
39. Teasdale G, Jennett B. Assessment of coma and impaired consciousness. A practical scale. Lancet. 1974;2:81–84.
40. Dikmen SS, Ross BL, Machamer JE, Temkin NR. One year psychosocial outcome in head injury. J Int Neuropsychol Soc. 1995;1:67–77. 10.1017/S1355617700000126.
41. King NS, Crawford S, Wenden FJ, Moss NE, Wade DT. The rivermead post concussion symptoms questionnaire: a measure of symptoms commonly experienced after head injury and its reliability. J Neurol. 1995;242:587–92. 10.1007/BF00868811.
42. Mosher JC, Leahy RM, Lewis PS. EEG and MEG: forward solutions for inverse methods. IEEE Trans Biomed Eng. 1999;46:245–59. 10.1109/10.748978.
43. Huang MX, Song T, Hagler DJ Jr, Podgorny I, Jousmaki V, Cui L, Gaa K, Harrington DL, Dale AM, Lee RR, et al. A novel integrated MEG and EEG analysis method for dipolar sources. Neuroimage. 2007;37:731–48. 10.1016/j.neuroimage.2007.06.002.
44. Huang M-X, Huang CW, Robb A, Angeles A, Nichols SL, Baker DG, Song T, Harrington DL, Theilmann RJ, Srinivasan R, et al. MEG source imaging method using fast L1 minimum-norm and its applications to signals with brain noise and human resting-state source amplitude images. Neuroimage. 2014;84:585–604. 10.1016/j.neuroimage.2013.09.022.
45. Ou W, Golland P, Hamalainen M. A distributed spatio-temporal EEG/MEG inverse solver. Med Image Comput Comput Assist Interv. 2008;11:26–34.
46. Haufe S, Tomioka R, Dickhaus T, Sannelli C, Blankertz B, Nolte G, Muller KR. Large-scale EEG/MEG source localization with spatial flexibility. Neuroimage. 2011;54:851–59. 10.1016/j.neuroimage.2010.09.003.
47. Huang CW, Huang M-X, Ji Z, Swan AR, Angeles AM, Song T, Huang JW, Lee RR. High-resolution MEG source imaging approach to accurately localize Broca's area in patients with brain tumor or epilepsy. Clin Neurophysiol. 2016;127:2308–16. 10.1016/j.clinph.2016.02.007.
48. Benjamini Y, Hochberg Y. Controlling the false positive rate: a prectical and powerful approach to multiple testing. J R Stat Soc Series B. 1995;57:289–300.
49. May A. Neuroimaging: visualising the brain in pain. Neurol Sci. 2007;28(Suppl 2):S101–107. 10.1007/s10072-007-0760-x.
50. May A, Bahra A, Büchel C, Frackowiak RS, Goadsby PJ. Hypothalamic activation in cluster headache attacks. The Lancet. 1998;352:275–78. 10.1016/S0140-6736(98)02470-2.
51. Qiu E, Wang Y, Ma L, Tian L, Liu R, Dong Z, Xu X, Zou Z, Yu S. Abnormal brain functional connectivity of the hypothalamus in cluster headaches. PLoS ONE. 2013;8:e57896. 10.1371/journal.pone.0057896.
52. Sánchez Del Rio M, Alvarez Linera J. Functional neuroimaging of headaches. Lancet Neurol. 2004;3:645–51. 10.1016/S1474-4422(04)00904-4.
53. Schankin CJ, Goadsby PJ. Mapping the brain in primary headache disorders. In: Toga AW, ed. Brain mapping. Waltham: Academic Press, 2015;1123–33.
54. Sun W, Deng A, Jayaram A, Gibson B. Noise exposure enhances auditory cortex responses related to hyperacusis behavior. Brain Res. 2012;1485:108–16. 10.1016/j.brainres.2012.02.008.
55. Arnsten AFT, Raskind MA, Taylor FB, Connor DF. The effects of stress exposure on prefrontal cortex: translating basic research into successful treatments for post-traumatic stress disorder. Neurobiol Stress. 2015;1:89–99. 10.1016/j.ynstr.2014.10.002.
56. Assenza G, Pellegrino G, Tombini M, Di Pino G, Di Lazzaro V. Wakefulness delta waves increase after cortical plasticity induction. Clin Neurophysiol. 2015;126:1221–27. 10.1016/j.clinph.2014.09.029.
57. Tecchio F, Pasqualetti P, Zappasodi F, Tombini M, Lupoi D, Vernieri F, Rossini PM. Outcome prediction in acute monohemispheric stroke via magnetoencephalography. J Neurol. 2007;254:296–305. 10.1007/s00415-006-0355-0.
58. Morawska MM, Büchele F, Moreira CG, Imbach LL, Noain D, Baumann CR. Sleep modulation alleviates axonal damage and cognitive decline after rodent traumatic brain injury. J Neurosci. 2016;36:3422–29. 10.1523/JNEUROSCI.3274-15.2016.
59. Xie L, Kang H, Xu Q, Chen MJ, Liao Y, Thiyagarajan M, O'Donnell J, Christensen DJ, Nicholson C, Iliff JJ, et al. Sleep drives metabolite clearance from the adult brain. Science. 2013;342:373–77. 10.1126/science.1241224.
60. Mander BA, Marks SM, Vogel JW, Rao V, Lu B, Saletin JM, Ancoli-Israel S, Jagust WJ, Walker MP. β-amyloid disrupts human NREM slow waves and related hippocampus-dependent memory consolidation. Nat Neurosci. 2015;18:1051–57. 10.1038/nn.4035.
61. Abd Hamid AI, Gall C, Speck O, Antal A, Sabel BA. Effects of alternating current stimulation on the healthy and diseased brain. Front Neurosci. 2015;9:391. 10.3389/fnins.2015.00391.
62. Antal A, Herrmann CS. Transcranial alternating current and random noise stimulation: possible mechanisms. Neural Plast. 2016;2016:3616807. 10.1155/2016/3616807.
63. Fertonani A, Miniussi C. Transcranial electrical stimulation: what we know and do not know about mechanisms. Neuroscientist. 2017, Vol. 23(2):109–123.
64. Paulus W. Transcranial electrical stimulation (tES - tDCS; tRNS, tACS) methods. Neuropsychol Rehabil. 2011;21:602–17. 10.1080/09602011.2011.557292.
65. Niedermeyer E, Lopes Da Silva FH. Electroencephalography: basic principles, clinical applications, and related fields. Philadelphia,

Baltimore, New York, London, Buenos Aires, Hong Kong, Sydney, Tokyo: Lippincott Williams & Wilkins, 2005.
66. Cohen D, Schlapfer U, Ahlfors S, Hamalainen M, Halgren E. New six-layer magnetically-shielded room for MEG. In: Nowak HHJ, Giebler F, eds. Proceedings of the 13th International Conference on Biomagnetism. Jena (Germany): VDE Verlag; 2002;919–21.
67. Taulu S, Simola J, Kajola M. MEG recordings of DC fields using the signal space separation method (SSS). Neurol Clin Neurophysiol. 2004;2004:35.
68. Taulu S, Kajola M, Simola J. Suppression of interference and artifacts by the signal space separation method. Brain Topogr. 2004;16:269–75. 10.1023/B:BRAT.0000032864.93890.f9.
69. Song T, Gaa K, Cui L, Feffer L, Lee RR, Huang M. Evaluation of signal space separation via simulation. Med Biol Eng Comput. 2008;46:923–32. 10.1007/s11517-007-0290-y.
70. Hyvarinen A, Oja E. Independent component analysis: algorithms and applications. Neural Netw. 2000;13:411–30. 10.1016/S0893-6080(00)00026-5.
71. Hyvarinen A. Fast and robust fixed-point algorithms for independent component analysis. IEEE Trans Neural Netw. 1999;10:626–34. 10.1109/72.761722.
72. Jovicich J, Czanner S, Greve D, Haley E, Van Der KA, Gollub R, Kennedy D, Schmitt F, Brown G, Macfall J, et al. Reliability in multi-site structural MRI studies: effects of gradient non-linearity correction on phantom and human data. Neuroimage. 2006;30:436–43. 10.1016/j.neuroimage.2005.09.046.
73. Shen X, Tokoglu F, Papademetris X, Constable RT. Groupwise whole-brain parcellation from resting-state fMRI data for network node identification. Neuroimage. 2013;82:403–15. 10.1016/j.neuroimage.2013.05.081.

Appendix 1. Technical Details of MEG and MRI Data Acquisition and Pre-processing

MEG Data Acquisition and Signal Pre-processing to Remove Artefacts

Resting-state MEG data were collected using the VectorView™ whole-head MEG system (Elekta-Neuromag, Helsinki, Finland) with 306 MEG channels. Participants were seated in upright position inside a multi-layer magnetically-shielded room (IMEDCO-AG) (66) at the UCSD MEG Center. For each participant, two 5-minute sessions with eyes closed were acquired. The participants were instructed to empty their minds and to avoid moving their eyes. Data were sampled at 1000 Hz and were run through a high-pass filter with a 0.1 Hz cut-off, and a low-pass filter with a 330 Hz cut-off. Eye blinks and eye movements were monitored using two pairs of bipolar electrodes with one pair placed above and below the left eye, and the other pair placed on the two temples. Heart signals were monitored with another pair of bipolar electrodes. Precautions were taken to ensure head stability: foam wedges were inserted between the participant's head and the inside of the unit, and a Velcro strap was placed under the participant's chin and anchored in superior and posterior axes. Head movement across different sessions was about 2–3 mm on average.

To help ensure that participants were alert during the MEG recordings, prior to each of the study sessions, they completed a questionnaire about the number of hours they slept the previous night, how rested they felt, and if there was any reason that they might not be attentive and perform to the best of their abilities (due to headache, pain, etc.). Participants were scheduled early in the day to avoid fatigue from performing daily activities. The amount of alpha band oscillations, which is consistently associated with tonic alertness, was also monitored online to gauge the cognitive state of participants. Participants were viewed on a camera, which also allowed for monitoring alertness of each participant.

MEG eyes-closed data were first run through MaxFilter, also known as signal space separation (67–69), to remove external interferences (e.g. magnetic artefacts due to metal objects, strong cardiac signals, environment noises, etc.). Next, residual artefacts near the sensor array due to eye movements and residual cardiac signals were removed using Independent Component Analysis using Fast-ICA (http://research.ics.aalto.fi/ica/fastica/) (70,71). The waveforms associated with top independent components (ICs) were examined by an experienced MEG data analyst, along with ECG and EOG signals. ICs associated with eye blinks, eye movements, heartbeats, and other artefacts were removed.

Structural MRI, MEG-MRI Registration, BEM Forward Calculation

Structural MRI of the participant's head was collected using a General Electric 1.5T Excite MRI scanner. The acquisition contains a standard high-resolution anatomical volume with a resolution of $0.94 \times 0.94 \times 1.2$ mm^3 using a T1-weighted 3D-IR-FSPGR pulse sequence. Scanner-related imaging distortions were corrected using a gradient non-linearity correction approach (72). To co-register the MEG with MRI coordinate systems, three anatomical landmarks (i.e. left and right pre-auricular points, and nasion) were measured for each participant using the Probe Position Identification system (Polhemus, USA). By identifying the same three points on the participant's MR images using MRILAB (Elekta/Neuromag), a transformation matrix involving both rotation and translation between the MEG and MR coordinate systems was generated. To increase the reliability of the MEG-MR co-registration, at least 150 points on the scalp were digitized with the Polhemus system, in addition to the three landmarks, and those points were co-registered onto the scalp surface of the MR images. The T1-weighted images were also used to extract the brain volume and innermost skull surface (SEGLAB software developed by Elekta/Neuromag). Realistic Boundary Element Method (BEM) head model was used for MEG forward calculation (42,43). The BEM mesh was constructed by tessellating the inner skull surface from the T1-weighted MRI into ~6000 triangular elements with ~5 mm size. A cubic source grid with 5 mm size covering cortical and subcortical GM areas based on FCONN brain parcellation (73) was created. Such a source grid was used for calculating the MEG gain (i.e. lead-field) matrix, which leads to a grid with ~10,000 nodes covering the whole brain. Then, the source grid was combined with the BEM mesh in the MRI coordinate for the BEM forward calculation.

Appendix 2. Chart of Iasis 5.0 Offset Values Applied

Name	Time	Hz, Offset
Genesis		
Start	2	14
FB1	5	7
FB2	5	3.3
FB3	5	6.6
FB4	5	10
FB5	5	7
Balanced Energy		
Start	3	3.33
FB1	2	21
FB2	2	13
FB3	2	2.6
FB4	2	2.4
FB5	2	0.7
FB6	2	0.3
FB7	2	−0.3
FB8	2	−1.8
FB9	2	11
FB10	2	4.83
FB11	2	13
FB12	2	4.78
FB13	2	11
Activation		
Start	3	14
FB1	4	7
FB2	3	7.8
FB3	2	14
FB4	2	3.9
FB5	1	5
FB6	1	6
FB7	1	7
FB8	1	8
FB9	1	9
FB10	1	10
FB11	1	11
FB12	1	12
FB13	1	13
FB14	1	14
FB15	1	7